Concluding Remarks

The vibration control of large flexible space structures with repeated or closely spaced frequencies is a challenging problem. Most of the previous investigations have focused on the qualitative analysis. Although some criteria for model reduction, such as frequency criterion and controllability and observability criteria, have been considered in the past, they cannot deal with vibration modes with repeated frequency. The contribution of the present paper is the use of the singular-value decomposition of the input matrix B_0 in defining controllability. This approach is also used to define the observability on the basis of duality. Using this method, the concepts of controllable principal modes and observable principal modes are introduced. These concepts describe the structures of controllability and observability for the subspace of the repeated-frequency modes in a more clear fashion. They are of practical importance for model reduction, sensor/actuator placement, and placement of exciters/sensors for modal parameter identification.

Acknowledgment

This study was supported by the National Natural Science Foundation of China.

References

[1]Hamdan, A. M. A., and Nayfeh, A. H., "Measures of Modal Controllability and Observability for First- and Second-Order Linear Systems," *Journal of Guidance, Control, and Dynamics*, Vol. 12, No. 3, 1989, pp. 421–428.

[2]Porter, B., and Crossley, R., *Modal Control Theory and Applications*, Taylor & Francis, 1972.

[3]Laub, A. J., and Arnold, W. F., "Controllability and Observability Criteria for Multivariable Linear Second-Order Models," *IEEE Transactions on Control*, Vol. AC-29(2), 1984, pp. 163–165.

[4]Hughes, P. C., and Skelton, R. E., "Controllability and Observability of Linear Matrix Second-Order Systems," *ASME Journal of Applied Mechanics*, Vol. 47, 1980, pp. 415–420.

[5]Gregory, C. Z., Jr., "Reduction of Large Flexible Spacecraft Models Using Internal Balancing Theory," *Journal of Guidance Control and Dynamics*, Vol. 7, No. 6, 1984, pp. 725–732.

[6]Williams, T., "Closed-Form Grammians and Model Reduction for Flexible Space Structures," *IEEE Transactions on Automatic Control*, Vol. 35, No. 3, 1990, pp. 372–382.

Automatic Formation Flight Control

M. Pachter,* J. J. D'Azzo,† and J. L. Dargan‡
Air Force Institute of Technology, Wright-Patterson AFB, Ohio 45433

I. Introduction

THE formation flight control problem is addressed in this Note. The automatic control of a two-aircraft flight, such that the formation's initial geometry is preserved during heading change and speed change maneuvers, is considered. A typical leader/wingman "diamond" formation is considered (see Fig. 1).

From an operational point of view, and in line with the current operational practice of manually flown formation flights, it is advantageous to stipulate a leader/follower concept for automatic formation flight control. This envisages a follower, i.e., the wingman, equipped with a "formation-hold" autopilot. Thus, the wingman (W) is controlled by the formation-hold autopilot.

Received Aug. 3, 1992; revision received March 25, 1994; accepted for publication May 23, 1994. This paper is declared a work of the U.S. government and is not subject to copyright protection in the United States.

*Associate Professor, Department of Electrical and Computer Engineering.

†Professor and Department Head, Department of Electrical and Computer Engineering.

‡Captain, U.S. Air Force, Department of Electrical and Computer Engineering.

The aircraft are modeled as first-order dynamic systems. It is assumed that the position of the leader (L) relative to W is available to W, and a W control system is developed for the automatic maintenance of the formation. The above-mentioned automatic formation flight control system (FFCS) is referred to as the formation-hold autopilot. Thus, W is able to maintain his or her position relative to L (station keeping), in the face of maneuvers by L. In addition, L can "command" a change (Δx_r, Δy_r) in the formation's parameters, i.e., a change in the L-W lateral and longitudinal separation (x_r, y_r). This prompts the formation-hold autopilot to command W to execute a maneuver in order to effect the commanded change. Hence, L literally "leads," or drives, the formation.

Concerning the measurements available for feedback, it is imperative that the perturbations in W's position in the formation, x and y, be available to the W collocated formation-hold autopilot. The additional information of heading error and speed error, viz., the availability of the measurements of leader-wingman heading and speed differentials, significantly improve the formation-hold autopilot's performance.

An early U.S. Army formation flight control system feasibility study was conducted in 1965. It concluded that a FFCS would relieve the pilot of the burdensome tasks required during formation flight and would greatly enhance formation flying performance (Ref. 1, p. 148). Recently, a preliminary FFCS study was performed by Rohs,[2] who considered diamond and trail formations of like and dissimilar aircraft. The work presented herein is based on the thesis research performed by Dargan[3] and Dargan et al.[4] In the present paper, a rotating frame of reference, affixed to W instantaneous position, is employed. The formation control problem is then modeled by a nonlinear dynamic system, which is developed in Sec. II. In Sec. III, the dynamic system is linearized about its initial steady-state condition. A decomposition principle is at work in the FFCS, which greatly facilitates the synthesis of the linear proportional-plus-integral (PI) controller. The crucial decomposition of the FFCS is performed in Sec. IV, followed by the analysis of the y and x channel control systems in Sec. V. The decomposition-based control design concept is very much in line with Porter and Bradshaw's modal (decomposition) method.[5,6] Finally, the linear plant model is employed to design a linear PI wing controller, which is the formation-hold autopilot. The formation-hold control concept is illustrated in Fig. 2 in Sec. V. The performance of the formation-hold autopilot is gauged by exercising the simulation with maneuvers performed by L (e.g., changes in L heading and speed). In addition, changes in the formation's parameters and formation changes can be commanded. An example of these simulation results is presented in Sec. VI. Concluding remarks are contained in Sec. VII.

II. Formation Flight Control Modeling

A. Main Assumptions

In the formation flight control problem analysis, it is tacitly assumed that standard autopilot loops have been closed around *each* aircraft in the formation. Hence, the aircraft are "flown" by controlling their respective Mach-hold and course-hold autopilots' reference signals.

B. Aircraft Dynamics

It is thus assumed that the following two decoupled autopilots are in place: (1) heading-hold autopilot, which accepts a (small) heading change command ψ_c in the heading ψ without affecting the aircraft's airspeed, and (2) Mach-hold autopilot, which accepts a (small) speed change command ΔV_c in speed V without affecting the aircraft's altitude. These decoupling assumptions implicitly presuppose coordinated throttle, stick, aileron, and rudder control in the first autopilot and coordinated stick and throttle control in the second autopilot. Furthermore, the heading dynamics and the attendant speed response of the autopilot controlled L and W aircraft are first order, respectively. Finally, realism-enhancing rate saturation nonlinearities are included in the above models.

The (linearized) dynamics are

$$\dot{\psi}_W = -\frac{1}{\tau_{\psi_W}}\psi_W + \frac{1}{\tau_{\psi_W}}\psi_{W_c} \tag{1}$$

$$\dot{V}_W = -\frac{1}{\tau_{V_W}} V_W + \frac{1}{\tau_{V_W}} V_{W_c} \tag{2}$$

$$\dot{\psi}_L = -\frac{1}{\tau_{\psi_L}} \psi_L + \frac{1}{\tau_{\psi_L}} \psi_{L_c} \tag{3}$$

$$\dot{V}_L = -\frac{1}{\tau_{V_L}} V_L + \frac{1}{\tau_{V_L}} V_{L_c} \tag{4}$$

where the L aircraft/autopilot system is modeled by Eqs. (3) and (4) and the W aircraft/autopilot system is modeled by Eqs. (1) and (2). The envisaged formation flight control (i.e., the formation-hold) autopilot entails an additional outer loop, closed around the formation, which drives the above-mentioned, standard, inner loop autopilots of the W aircraft. The latter, it is recalled, are controlled by (ψ_{W_c}, V_{W_c}). Finally, the formation-hold closed-loop system is driven by the exogenous input $(\psi_{L_c}, \Delta V_{L_c})$, which is the leader's control.

C. Kinematics

The planar situation is considered. A (rotating) frame of reference, centered at W instantaneous position and with the x axis aligned with W instantaneous velocity vector $\boldsymbol{V}_W$, is used; the y axis is along W starboard wing. Thus, L's position relative to W is (x, y). This is illustrated in Fig. 1. Also, without loss of generality, the X axis of the inertial reference frame is chosen to be aligned with the initial quiescent velocity vector of the formation, which is due north (so that the heading perturbation $\Delta\psi = \psi$). The quiescent formation's velocity is V_n.

With the notation shown in Fig. 1, the equations of relative motion of the L-W formation are found to be

$$\frac{\mathrm{d}x}{\mathrm{d}t} = \dot{\psi}_W y - V_W + V_L \cos\psi_e \tag{5}$$

$$\frac{\mathrm{d}y}{\mathrm{d}t} = -\dot{\psi}_W x + V_L \sin\psi_e \tag{6}$$

where the "heading error"

$$\psi_e \equiv \psi_L - \psi_W \tag{7}$$

Inserting the expression for W's turning rate [Eq. (1)] into the kinematic equations (5) and (6) yields

$$\frac{\mathrm{d}x}{\mathrm{d}t} = -\frac{y}{\tau_{\psi_W}} \psi_W - V_W + V_L \cos\psi_e + \frac{y}{\tau_{\psi_W}} \psi_{W_c} \tag{8}$$

$$\frac{\mathrm{d}y}{\mathrm{d}t} = \frac{x}{\tau_{\psi_W}} \psi_W + V_L \sin\psi_e - \frac{x}{\tau_{\psi_W}} \psi_{W_c} \tag{9}$$

Hence, the FFCS dynamics are given by Eqs. (1–4) and (7–9). Note that the exogenous leader control affects all the states of the plant, which is described by the augmented dynamic system (1–4) and (7–9).

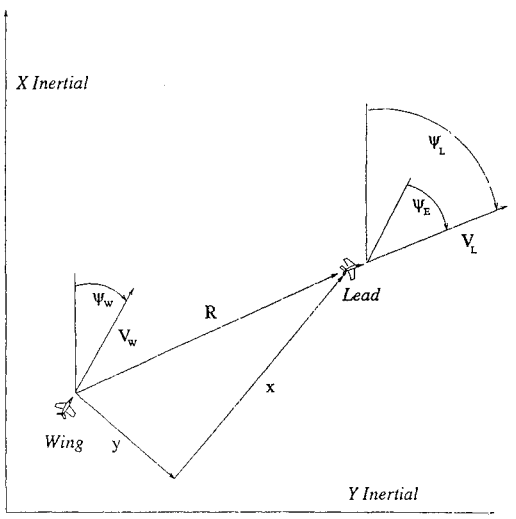

Fig. 1 Wing aircraft rotating reference frame.

III. Linearization

Upon linearizing the x and y equations of motion (8) and (9) and using Eq. (7), the linear time-invariant (LTI) FFCS comprised of Eqs. (10), (11), and (1–4) is obtained:

$$\dot{x} = -\frac{y_r}{\tau_{\psi_W}} \psi_W - V_W + V_L + \frac{y_r}{\tau_{\psi_W}} \psi_{W_c} \tag{10}$$

$$\dot{y} = \left(\frac{x_r}{\tau_{\psi_W}} - V_n\right) \psi_W + V_n \psi_L - \frac{x_r}{\tau_{\psi_W}} \psi_{W_c} \tag{11}$$

Here, x and y are perturbation variables, i.e., $x - x_r \to x$ and $y - y_r \to y$; similarly, $V_L - V_n = \Delta V_L \to V_L$ and $V_W - V_n = \Delta V_W \to V_W$. The state vector is $(x, y, \psi_W, V_W, \psi_L, V_L)' (\in R^6)$. Also, it is important to realize that, in the FFCS, the control vector is $(\psi_{W_c}, V_{W_c})' (\in R^2)$. Furthermore, L control $(\psi_{L_c}, V_{L_c})' (\in R^2)$ is an additional exogenous input to the FFCS (10), (11), and (1–4) in the current formation-hold autopilot design context and is considered a *disturbance* signal exciting the system. Thus, the formation-hold autopilot's task is to "fight," i.e., to reject, this disturbance.

IV. Decomposition

The FFCS six-dimensional state vector is rearranged and partitioned as follows: x, V_W, V_L and y, ψ_W, ψ_L.

Thus, the following two dynamic systems, each of dimension 3 and referred to as the x channel and the y channel, respectively, are obtained as

$$\dot{x} = -V_W + V_L - \frac{y_r}{\tau_{\psi_W}} \psi_W + \frac{y_r}{\tau_{\psi_W}} \psi_{W_c} \tag{12}$$

$$\dot{V}_W = -\frac{1}{\tau_{V_W}} V_W + \frac{1}{\tau_{V_W}} V_{W_c} \tag{13}$$

$$\dot{V}_L = -\frac{1}{\tau_{V_L}} V_L + \frac{1}{\tau_{V_L}} V_{L_c} \tag{14}$$

and

$$\dot{y} = \left(\frac{x_r}{\tau_{\psi_W}} - V_n\right) \psi_W + V_n \psi_L - \frac{x_r}{\tau_{\psi_W}} \psi_{W_c} \tag{15}$$

$$\dot{\psi}_W = -\frac{1}{\tau_{\psi_W}} \psi_W + \frac{1}{\tau_{\psi_W}} \psi_{W_c} \tag{16}$$

$$\dot{\psi}_L = -\frac{1}{\tau_{\psi_L}} \psi_L + \frac{1}{\tau_{\psi_L}} \psi_{L_c} \tag{17}$$

Hence, the system matrices are

$$A = \left[\begin{array}{ccc|ccc} 0 & -1 & 1 & 0 & -\frac{y_r}{\tau_{\psi_W}} & 0 \\ 0 & -\frac{1}{\tau_{V_W}} & 0 & 0 & 0 & 0 \\ 0 & 0 & -\frac{1}{\tau_{V_L}} & 0 & 0 & 0 \\ \hline 0 & 0 & 0 & 0 & \frac{x_r}{\tau_{\psi_W}} - V_n & V_n \\ 0 & 0 & 0 & 0 & -\frac{1}{\tau_{\psi_W}} & 0 \\ 0 & 0 & 0 & 0 & 0 & -\frac{1}{\tau_{V_L}} \end{array}\right]$$

$$B = \begin{bmatrix} \frac{y_r}{\tau_{\psi_W}} & 0 \\ 0 & \frac{1}{\tau_{V_W}} \\ 0 & 0 \\ - & - \\ -\frac{x_r}{\tau_{\psi_W}} & 0 \\ \frac{1}{\tau_{\psi_W}} & 0 \\ 0 & 0 \end{bmatrix}$$

and the disturbance input matrix is

$$\Gamma = \begin{bmatrix} 0 & 0 \\ 0 & 0 \\ 0 & \frac{1}{\tau_{V_L}} \\ - & + \; - \\ 0 & 0 \\ 0 & 0 \\ \frac{1}{\tau_{\psi_L}} & 0 \end{bmatrix}$$

Thus,

$$A = \begin{bmatrix} A_{11} & A_{12} \\ 0 & A_{22} \end{bmatrix} \qquad B = \begin{bmatrix} B_1 \\ B_2 \end{bmatrix}$$

$$\Gamma = \begin{bmatrix} 0 & \Gamma_1 \\ \Gamma_2 & 0 \end{bmatrix}$$

and the accordingly partitioned state vector is $(X_1, X_2)'$. Here, the 3×3 blocks are

$$A_{11} = \begin{bmatrix} 0 & -1 & 1 \\ 0 & -\frac{1}{\tau_{V_W}} & 0 \\ 0 & 0 & -\frac{1}{\tau_{V_L}} \end{bmatrix} \qquad A_{12} = \begin{bmatrix} 0 & -\frac{y_r}{\tau_{\psi_W}} & 0 \\ 0 & 0 & 0 \\ 0 & 0 & 0 \end{bmatrix}$$

$$A_{22} = \begin{bmatrix} 0 & \frac{x_r}{\tau_{\psi_W}} - V_n & V_n \\ 0 & -\frac{1}{\tau_{\psi_W}} & 0 \\ 0 & 0 & -\frac{1}{\tau_{V_L}} \end{bmatrix}$$

In addition,

$$B_1 = \begin{bmatrix} \frac{y_r}{\tau_{\psi_W}} & 0 \\ 0 & \frac{1}{\tau_{V_W}} \\ 0 & 0 \end{bmatrix} \qquad B_2 = \begin{bmatrix} -\frac{x_r}{\tau_{\psi_W}} & 0 \\ \frac{1}{\tau_{\psi_W}} & 0 \\ 0 & 0 \end{bmatrix}$$

$$\Gamma_1 = \begin{bmatrix} 0 \\ 0 \\ \frac{1}{\tau_{V_L}} \end{bmatrix} \qquad \Gamma_2 = \begin{bmatrix} 0 \\ 0 \\ \frac{1}{\tau_{\psi_L}} \end{bmatrix}$$

It becomes apparent from the partitioned structure of the A, B, and Γ system matrices that the following decomposition principle applies: The three-state y channel, whose state $X_2 = (y, \psi_W, \psi_L)$, is decoupled from the three-state x channel. In other words, the y- and x-channel controllers can be designed independently.

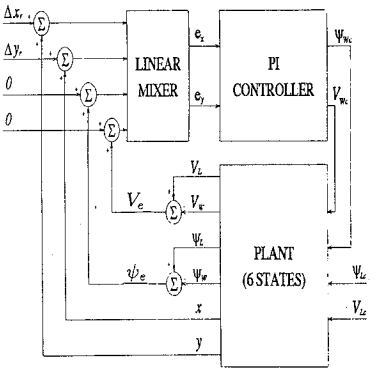

Fig. 2 Linear control synthesis model.

V. Control Design

The y channel is controlled by the single input ψ_{W_c}. The disturbance signal in the y channel is ψ_{L_c}. Also, in the y channel, the two measured outputs available for feedback are the heading error $\psi_e = \psi_L - \psi_W$ and the lateral separation error y; viz., the output matrix is

$$C_2 = \begin{bmatrix} 0 & -1 & 1 \\ 1 & 0 & 0 \end{bmatrix}$$

Hence, the y-channel dynamics are

$$\dot{X}_2 = A_{22}X_2 + b_2\psi_{W_c} + \Gamma_2\psi_L \tag{18}$$

where the input vector is

$$b_2 \equiv \left[-\frac{x_r}{\tau_{\psi_W}}, \frac{1}{\tau_{\psi_W}}, 0 \right]' \tag{19}$$

and the disturbance input vector is

$$\Gamma_2 = \left[0, 0, \frac{1}{\tau_{\psi_L}} \right]' \tag{20}$$

Next, a generalized y-channel scalar error signal is introduced; viz., the lateral position error and the heading error are *mixed* according to

$$e_y \equiv k_y y + k_\psi \psi \tag{21}$$

and a linear PI control law for the y channel is proposed,

$$\psi_{W_c} = K_{y_P} e_y + K_{y_I} \int_0^t e_y \, dt \tag{22}$$

Similarly, in the x channel, the error signal is

$$e_x \equiv k_x x + k_V e_V \tag{23}$$

and a linear PI control law is proposed,

$$V_{W_c} = K_{x_P} e_x + K_{x_I} \int_0^t e_x \, dt \tag{24}$$

The controller's gains are determined using a pole placement technique (for more details, see, e.g., Ref. 7).

The formation control concept is illustrated in Fig. 2.

VI. Performance Evaluation

The FFCS shown in Fig. 2 is simulated using MATRIX$_x$-System Build. The aircraft are flying in a "diamond" leader-wingman formation with a spacing $x = 500$ ft and $y = 200$ ft. The formation is commanded a heading change of 45 deg. In this case, the lead aircraft is turning into the wing aircraft. The time response plots of Fig. 3 illustrate that, as the wing aircraft tracks the heading response of the lead aircraft, transients in the formation spacing and the wing aircraft velocity occur. The closest separation between the aircraft during the maneuver is a safe 474 ft. However, as the transients die

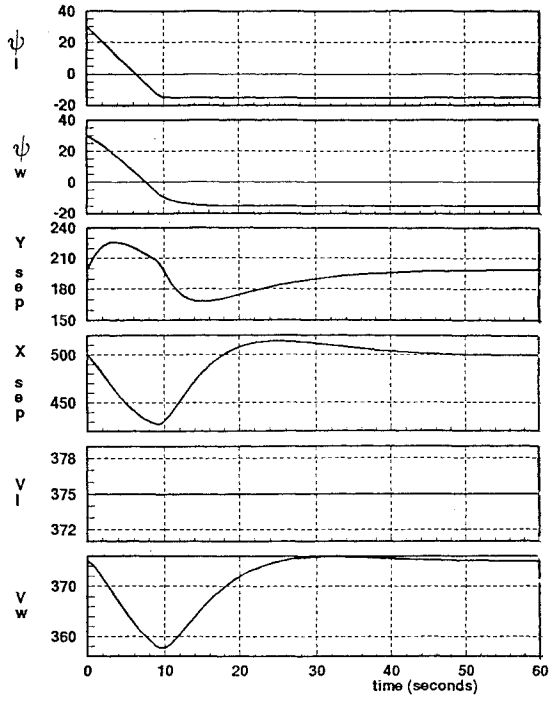

Fig. 3 Time response plots for diamond leader-wingman formation.

out, the initial formation velocity and the initial formation spacing are maintained in steady state. Therefore, the formation geometry is maintained after the heading change maneuver is completed and there is no danger of an L/W collision during the transition process.

VII. Conclusions

The control design problem of an automatic pilot for formation flight control has been analyzed and decomposed into two uncoupled linear single-input, two-output dynamic tracking control system design problems, which correspond to the y and x channels, respectively. This, in turn, results in the efficient design of a PI formation-hold autopilot that uses a mix of separation errors and maneuver errors. The formation-hold autopilot is an extension of the conventional heading-hold and Mach-hold autopilots. However, the formation control problem involves two flight vehicles and their accurate relative positions.

The formation flight control problem considered here is significant in view of its direct operational importance: It affords the automation of the coordination of a leader/wingman flight, the design of a robotic wingman, and the automatic control of aircraft during maneuvers such as aerial refueling. It is also interesting in view of the novel and nontrivial control theoretic problems that it poses.

References

[1]Wellinger, D., "Army Formation Flight Study: Final Report," Contract No. DA-36-039-ACM-03367(E), Radio Corporation of America, Burlington, MA, Feb. 1965.

[2]Rohs, P. R., "A Fully Coupled, Automated Formation Control System for Dissimilar Aircraft in Maneuvering, Formation Flight," M.S. Thesis, AFIT/GE/ENG/91M-03, Air Force Inst. of Technology, Wright-Patterson AFB, OH, March 1991.

[3]Dargan, J. L., "Proportional Plus Integral Control of Aircraft for Automated Maneuvering Formation Flight," M.S. Thesis, AFIT/GE/ENG/ 91D-14, Air Force Inst. of Technology, Wright-Patterson AFB, OH, Dec. 1991.

[4]Dargan, J. J., Pachter, M., and D'Azzo, J. J., "Automatic Formation Flight Control," *Proceedings of the AIAA Guidance, Navigation and Control Conference* (Hilton Head, SC), AIAA, Washington, DC, 1992, pp. 836–857 (AIAA Paper No. 92-4473).

[5]Porter, B., and Bradshaw, A., "Design of Linear Multivariable Continuous-Time Tracking Systems," *International Journal of System Science*, Vol. 5, 1974, pp. 1155–1164.

[6]Porter, B., and Bradshaw, A., "Singular Pertubation Methods in the Design of Tracking Systems Incorporating Inner-Loop Compensators and High-Gain Error-Actuated Controllers," *International Journal of System Science*, Vol. 12, 1981, pp. 1193–1205.

[7]Buzogany, L. E., Pachter, M., and D'Azzo, J. J., "Automated Control of Aircraft in Formation Flight," *Proceedings of the AIAA Guidance, Navigation and Control Conference* (Monterey, CA), AIAA, Washington, DC, 1993, pp. 1349–1370 (AIAA Paper No. 93-3852).

Drag Function Modeling for Air Traffic Simulation

Mark R. Anderson*
Virginia Polytechnic Institute and State University, Blacksburg, Virginia 24061
and
Daniel E. Schab†
Naval Air Warfare Center, Orlando, Florida 32826

Introduction

In most modern aircraft training simulators, many aircraft are being flown simultaneously to mimic surrounding air traffic. For combat simulators, the flight performance fidelity of the aircraft traffic or threat environment is particularly important for effective combat tactics training. The air traffic models must also be very simple so that a minimum amount of computational power is used during these real-time simulations.

Most air traffic models in use today have been developed by piecing together manufacturer's data into a simplified model of the aircraft. However, for many aircraft, data may be available in the form of performance charts. Excess power contours and energy maneuverability charts are estimated for many aircraft to make comparisons between different aircraft types. These performance predictions are a valuable source of information that can be used for air traffic simulation modeling.

This note offers a new approach to developing a drag function expression for commercial air traffic or combat aircraft threat models. The idea is to determine parameters of a simplified drag coefficient function so that the performance of the modeled aircraft closely matches that of the actual aircraft. The drag function parameters are varied using a form of parameter identification or multidimensional curve fitting. In other words, the parameters of the air traffic model drag function are actually extracted from performance data rather than estimated from wind tunnel data. Thus, the performance of the air traffic model will match the actual aircraft.

Drag Error Function Structure

Most air traffic models are based upon energy state equations of motion.[1–5] The excess power or rate of change of energy is given by

$$P_s = \frac{\mathrm{d}E}{\mathrm{d}t} = \frac{V(T-D)}{W} \tag{1}$$

where $E = h + V^2/2g$ is specific energy, h is altitude, V is velocity, W is weight, and P_s is excess power. The axial forces acting on the

Received Nov. 6, 1993; revision received April 8, 1994; accepted for publication April 14, 1994.

*Assistant Professor, Department of Aerospace and Ocean Engineering. Senior Member AIAA.

†Aerospace Engineer, Training Systems Division, Fighter Attack Branch. Member AIAA.